Bio-polyol chemical design for self-healing boronate ester gels by green oxyalkylation of organosolv lignin

Bram Jacobs[a,b], Ine Van Nieuwenhove[c], Sander Driesen[b], Pablo Reyes[d], Dagmar R. D'hooge[d,e], Geert-Jan Graulus[b], Katrien V. Bernaerts[f], An Verberckmoes[a*]

[a] Faculty of engineering and architecture, Department of Materials, Textiles and Chemical Engineering, Industrial Catalysis and Adsorption Technology (INCAT), Ghent University, Valentin Vaerwyckweg 1, 9000 Ghent, Belgium, An.Verberckmoes@ugent.be

[b] Hasselt University, Institute for Materials Research (imo-imomec), Biomolecule Design Group, Agoralaan (Building D), 3590 Diepenbeek, Belgium

[c] Brussels Health Campus, Erasmus Brussels University of Applied Sciences and Arts, Laarbeeklaan 121, 1090 Jette, Belgium

[d] Faculty of engineering and architecture, Department of Materials, Textiles and Chemical Engineering, Laboratory for Chemical Technology (LCT), Ghent University, Technologiepark 125, 9052 Zwijnaarde, Belgium

[e] Faculty of engineering and architecture, Department of Materials, Textiles and Chemical Engineering, Centre for Textile Science and Engineering (CTSE), Ghent University, Technologiepark 70a, 9052 Zwijnaarde, Belgium

[f] Sustainable Polymer Synthesis Group, Aachen-Maastricht Institute for Biobased Materials (AMIBM), Faculty of Science and Engineering, Maastricht University, Urmonderbaan 22, 6167 RD Geleen, the Netherlands

ABSTRACT – Lignin, the most abundant aromatic biopolymer, has a high potential as an alternative to fossil resources in the chemical industry. However, the non-uniformity of lignin is currently a drawback for high-end applications. In this work, glycerol carbonate being a green and safe cyclic carbonate was therefore applied in the oxyalkylation of organosolv lignin (weight average molecular weight of ≈ 8,300 g mol^{-1}; aliphatic OH content of ca. 2.61 mmol g^{-1}) to obtain a lignin-based polyol with solely aliphatic OH functionalities. The catalyst type, reaction temperature and time and additional solvents were evaluated in the oxyalkylation with optimal settings using K_2CO_3, 175 °C, 30 minute reaction time without any additional solvent to make a modified lignin with a weight average molecular weight of ca. 15,000 g mol^{-1} and an aliphatic OH content of ca. 4.59 mmol g^{-1}. To support mechanistic understanding it is shown that the carboxylic acid and phenolic hydroxyl functionalities are converted completely into 1,2-diols, while native aliphatic OH functionalities take at most slightly part in the modification reaction. Furthermore, upon the formation of vicinal diols, the functionalities partially react with glycerol carbonate by an internal transesterification into cyclic carbonate functionalities, this undesirable reaction being more dominant at lower temperatures. Notably, the performance of the oxyalkylation strategy is sufficient to crosslink the modified lignin with benzene-1,4-diboronic acid into a gel-like material with identical shear storage and loss moduli before destruction and immediately after destruction (for the lowest amount of crosslinker added = 1:1.15 diol/boronic acid functionalities molar ratio).

Keywords: organosolv lignin, oxyalkylation, glycerol carbonate, boronate ester, organogel

1. Introduction

Our society is heavily relying on fossil-based chemicals and materials, considering the wide use of oil-based fuels for transport, bulk and fine chemicals and the subsequent synthesis of polymers.[1] However, our fossil-based economy is under stress because of the devastating effects of climate change, the increased awareness of consumers for more sustainable products and the depletion of fossil resources.[2]–[5] The most abundant aromatic biopolymer lignin can play a pivotal role in the transition towards green alternatives for fossil resources.[6], [7] Lignins – as part of lignocellulose – are a non-edible feedstock with a wide variety of chemical functionalities (*e.g.* -COOH, -OH, $-OCH_3$ groups).[7]–[9] Since lignin is part of a complex structure with both cellulose and hemi-cellulose, a delignification technique is necessary to isolate lignin from the polysaccharides.[10]

While the commercially available lignins – *i.e.* technical lignins – have an altered chemical structure through pulping to isolate cellulose (*e.g.*, soda, Kraft and sulfite processes), the organosolv process, being part of the present work, is still under development. However, this process has gained increased attention as it regards lignin as valuable constituent instead of merely waste and maintains – not necessary, but possible, depending on the extraction conditions – the original lignin structure.[1], [11] Despite being still at pilot scale (≈ 125 kg lignin/batch or < 1000 ton per year)[12], [13], the organosolv process generates high purity lignin (potentially sulfur-free) and a concentrated sugar syrup which can be valorized into bio-ethanol.[14]–[17] However, lignin has a complex and irregular structure because of a varying monolignol composition and a variety of bonds which differ by plant species and the location in the plant, resulting in a recalcitrant polymer with a non-uniform reactivity.[18]

Since the majority of lignins is incinerated with energy recovery mainly in the Kraft process plant, only 2% is valorized.[19], [20] Extensive research has therefore been conducted to ameliorate the low valorization degree by depolymerizing lignins into fuels with high heating value, oligomers with a high phenolic OH content and valuable monomers such as vanillin.[5], [19] Another strategy is to apply lignin – as such – without any modification into resins as cheap filler material. While this strategy increases the bio-content, incorporating high amounts of lignins often results in loss of vital properties.[21] Because of the aromatic backbone structure and the phenolic OH functionalities, lignin is often regarded as a good substituent for phenol in phenol-formaldehyde (PF) resins with or without lignin modifications prior to PF-resin synthesis.[22]

An additional strategy consists of modifying existing functionalities or introducing new functionalities to synthesize a broader spectrum of polymers and resins from lignin feedstocks. Native alcohol functionalities can be converted into aliphatic OH (alOH) groups. This results in a

lignin with a more uniform functionality and, hence, a more uniform reactivity with a variety of application possibilities.[9], [19], [23]–[27] Historically, such modified substrates were obtained by the Williamson ether synthesis with alkyl halides and/or ring-opening of epoxides.[7], [26] Nevertheless, both approaches suffer from the absence of sustainable and safe reagents, with particular emphasis on the safety precautions involved upon handling ethylene oxide.[7], [28] Therefore, biodegradable cyclic carbonates are worthy green alternatives as etherification agents since they are non-volatile, have high boiling points and low odor levels.[29]–[31] Notably, Kühnel *et al.* applied four different cyclic carbonates (*i.e.* ethylene carbonate ($EtCO_3$), propylene carbonate ($PrCO_3$), butylene carbonate ($BuCO_3$) and glycerol carbonate ($GlyCO_3$) – see Figure 1) in the oxyalkylation at 170 °C of different lignins (Kraft, soda and organosolv) with 1,8-diazabicyclo[5.4.0]undec-7-ene (DBU).[29] They determined the order in which the cyclic carbonates decreased in reactivity, being $EtCO_3$ > $GlyCO_3$ > $PrCO_3$ > $BuCO_3$.

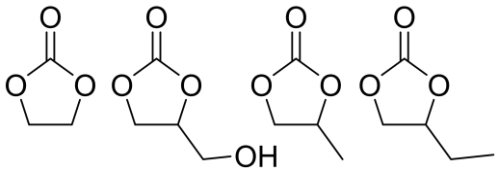

Figure 1 Cyclic carbonates with decreasing reactivity from left to right: ethylene carbonate ($EtCO_3$), glycerol carbonate ($GlyCO_3$), propylene carbonate ($PrCO_3$) and butylene carbonate ($BuCO_3$)

The mechanism of the oxyalkylation between lignin OH functionalities and cyclic carbonates is determined by the OH functionality.[30], [32]–[35] Figure S1 illustrates the oxyalkylation with $GlyCO_3$ which – in contrast to the other carbonates in Figure 1 – results in the conversion of 1 OH to 2 alOH groups. The phenolic OH (phOH) and COOH groups in lignins (resp. phenoxide and carboxylate ions after deprotonation) react with the less hindered (soft electrophile) methylene C-atom of $GlyCO_3$ which leads to a carbonate ester group at the end followed by the removal of CO_2 to obtain a vicinal diol.[36] In case the reaction occurs at the more hindered methine C-atom of $GlyCO_3$ – which is less likely to occur – a 1,3-diol is obtained.[31] Furthermore, the native (and less sterically hindered) alOH functionalities (in contrast with the phOH and COOH groups) favor to react with the electrophilic C-atom of the carbonyl bond in the absence of a decarboxylation step, resulting in a carbonate structure incorporated in the aliphatic chain. In addition to the reactions mentioned above, several side reactions (Figure 2) can occur such as the formation of polymer brushes via the homopolymerization of cyclic carbonates from the lignin backbone, the internal transesterification of 1,2-diols into cyclic carbonates and co-polymerization via transesterification via a carbonate structure.[36], [37]

Only a limited number of studies investigated the oxyalkylation for monomeric substrates such as Galletti *et al.* in which $GlyCO_3$ as etherifying agent reacted with phenol as monomeric substrate.[31] The use of both CH_3ONa and K_2CO_3 as catalyst resulted in high phenol conversions (95%) at 140 °C in a few hours. At 170 °C, the reaction rate increased but this high temperature also favored side reactions such as oligomerization by the formation of poly(1,2-glycerol carbonate) on top of the alOH groups. This side reaction was more noticeable with CH_3ONa than K_2CO_3 due to the stronger basicity.[31] Similar reaction temperatures were mentioned by Clements *et al*. with a temperature range of 150 °C – 200 °C for the oxyalkylation of alcohols with $EtCO_3$, while amines only require a temperature range of 100 °C – 150 °C.[30]

It should be stressed that by default studies give more theoretical insights in the reaction mechanism, however the translation from monomeric substrate to lignin remains still utmost challenging. Most studies use a technical lignin as substrate for the oxyalkylation with cyclic carbonates such as $EtCO_3$ and $PrCO_3$ and only a minority discusses the use of $GlyCO_3$ (often in combination with other cyclic carbonates).[29], [37]–[41] Kühnel *et al*. evaluated the use of $PrCO_3$ in the modification of organosolv lignin (OL) at 170 °C for 3h. $PrCO_3$ served both as reagent and as solvent as it was present in excess. The authors found high temperatures (T > 170 °C) in presence of alkaline catalysts to be favorable to avoid the formation of carbonate structures by alOH functionalities.[38] A follow-up study by Kühnel *et al*. investigated reaction temperatures lower than 170 °C.[33] At 100 °C, a high increase in weight average molecular weight (M_w) was observed which was likely caused by coupling reactions from terminal carbonate structures. At temperatures > 140 °C, there is a decrease in M_w and a narrower molecular weight distribution. In addition, Liu *et al*. searched for the optimal reaction conditions for the hydroxyethylation of phenolic OHs and COOHs in hardwood and softwood Kraft lignin by $EtCO_3$.[40] The modified lignin was more thermally stable and had a slightly lower glass transition temperature (T_g). A follow-up study focused on the suppression of unexpected structural changes in lignin (*e.g.* crosslinking) during the modification.[36], [42] Several softwood Kraft lignins were treated (100 °C – 120 °C for 0h – 6h) and the release of CO_2 was monitored through displacement of water. As these authors aimed for conversion of phOH and COOH functionalities, the CO_2 amount and production rate allow to determine whether the oxyalkylation was completed. Moreover, they discuss the newly formed alOH groups copolymerize with $EtCO_3$ resulting in carbonate linkages.

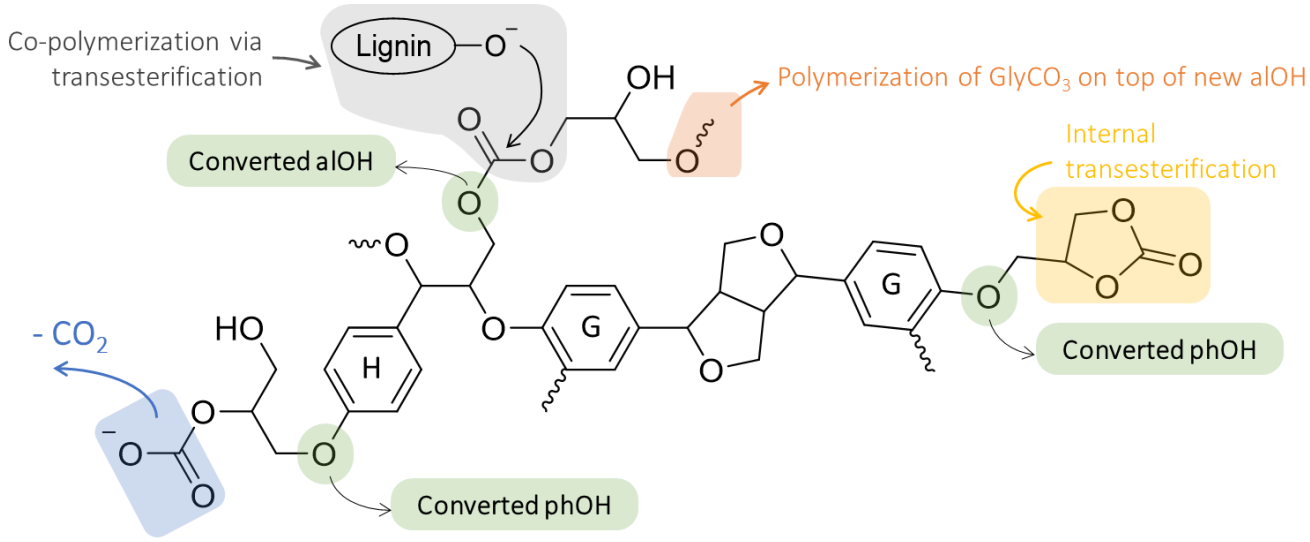

Figure 2 Oxyalkylation of different OH functionalities with $GlyCO_3$ and possible side reactions

In this study, the oxyalkylation of beech wood OL feedstock with $GlyCO_3$ into a polyol with uniform functionality was evaluated. In comparison with the other cyclic carbonates in Figure 1, $GlyCO_3$ has the highest boiling point of 354 °C, both $GlyCO_3$ and the degradation product glycerol are safe to use and have low toxicities, and only $GlyCO_3$ is able to increase the OH content by converting each OH group into a vicinal diol.[28], [31], [36] Furthermore, several $GlyCO_3$ synthesis pathways are valid such as the reaction of glycerol (which can be obtained from biodiesel production) and CO_2.[31], [43]

More in detail, the catalyst, reaction temperature and time and additional solvents were systematically varied to map the effect of these variables on the oxyalkylation process and to gain insights in the oxyalkylation mechanism and the synthesis of undesirable reaction products. The optimal conditions for the oxyalkylation – obtained in this study – were assessed by using an adaptation of the CHEM21 metrics toolkit made in earlier research.[7] In addition, as a proof-of-concept in this study, the modified lignin with vicinal diol functionalities was applied as a substrate in boronate ester gels. Dynamic covalent bonds – combining the strength of a covalent bond with the reversibility of non-covalent interactions with (or without) specific stimuli[44]–[46] – such as boronate esters are widely investigated in biomedical applications (initially as enzyme inhibitors)[44] such as chemical sensors for biomolecules containing diols (*e.g.* saccharides and adenosine triphosphate (ATP)), (glucose-responsive) drug delivery systems and hydrogels.[44], [47]–[51] The latter often acts as a drug delivery system as well whereby drugs are encapsulated in the hydrogel network and are subsequently released by an external stimulus. Moreover, the gel can be used as a wound dressing with inflammatory properties or can be applied in cell and tissue engineering.[52], [53] Thus, this study goes beyond the current state-of-the-art by in-depth focusing on $GlyCO_3$ as etherification agent, introducing modified lignin to the boronate ester-based gels and evaluating the gels self-healing capacity.

2. Materials and methods

2.1. Chemicals

The lignin was obtained from Fraunhofer CBP by an organosolv process of beech wood at 170 °C with ethanol/water and catalytic amounts of sulfuric acid. Prior to any experiment/analysis, the OL feedstock (with a determined moisture content of 3.0%) was milled and subsequently dried for 4h at 60 °C.

Deuterated chloroform ($CDCl_3$) stabilized with silver foil and deuterated dimethyl sulfoxide (DMSO-d_6) were purchased from Eurisotop. Dimethyl sulfoxide (DMSO, HPLC grade, 99.9+%) was bought from Biosolve. Tetrabutylammonium bromide (TBAB, 99+%) was purchased from Fischer Scientific. Acetone (99+%), hydrochloric acid (HCl, 37%), potassium carbonate (K_2CO_3, 99+%) and sodium hydroxide (NaOH) pellets were purchased from Chem-Lab. 1,8-diazabicyclo[5.4.0]undec-7-ene (DBU, 98%), 2-chloro-4,4,5,5-tetramethyl-1,3,2-dioxaphospholane (TMDP, 95%), anhydrous pyridine (99.8%), chromium(III)acetylacetonate ($Cr(acac)_3$, 97%), lithium bromide (LiBr, ≥99%), N-hydroxy-5-norbornene-2,3-dicarboxylic acid imide (NHND, 97%) and benzene-1,4-diboronic acid (≥95.0%) were purchased from Sigma-Aldrich. Ethylene carbonate ($EtCO_3$, >99.0%) and glycerol carbonate ($GlyCO_3$, >90.0%) were purchased from TCI Europe. GPC calibration was done with narrow polymethylmethacrylate standards (PMMA) ranging from 535 g mol^{-1} to 72,000 g mol^{-1} (Agilent Technologies, PSS Polymer Standards Service GmbH).

2.2. Oxyalkylation of beech wood OL

A two-neck round-bottom flask (25 mL) was filled with ± 0.50 g OL and 0.1 equivalents catalyst (with respect to the total OH content of OL). Subsequently, as shown in Figure S2, an excess of glycerol carbonate ($GlyCO_3$) (10 equivalents relative to the total OH content = sum of alOH, phOH and COOH functionalities) was transferred into the flask. Next, both necks were closed with rubber septa and the flask was flushed with N_2 for 1 minute. A needle connected to a balloon filled with N_2 was placed through the septum to counter the pressure build-up by CO_2 release during the reaction. The flask was then immersed in a pre-heated (120 °C – 200 °C) oil bath. After a two-minute pre-heat time (at the corresponding reaction temperature) at 800 rpm stirring speed, the stirring speed was set to 1600 rpm. After reaction, the flask was removed from the oil bath and the reaction medium was precipitated, while still being hot, in a 200 mL HCl (0.01 mol L^{-1}) solution (with high stirring

speed which created a visible vortex). The solution was stirred for another 30 minutes before filtering with a Buchner filter (Whatman grade 1) to avoid trapped $GlyCO_3$ in the precipitate. The solid lignin was scraped from the filter and transferred to a Petri dish and further dried in a drying oven (VWR) at 60 °C prior to analysis.

2.3. Developing a boronate ester gel

In brief, 0.20 g modified OL feedstock was dissolved together with an amount of benzene-1,4-diboronic acid in 1.00 mL DMSO in a 20 mL glass recipient. This mixture was homogenized with a magnetic stirring bar at 800 rpm for 10 minutes. Afterwards, an equal volume of aqueous 1 mol L^{-1} NaOH solution (1.00 mL) was added to the mixture. The mixture was stirred for 2 minutes and transferred to a circular shaped mold in PTFE in order to obtain disk-shaped gel samples.

2.3. Characterization techniques

2.3.2. Size exclusion chromatography

An Agilent 1260 Infinity II LC system was used for GPC analysis. The device was equipped with a Polargel-L guard column, two consecutive Polargel-L columns, a UV-VIS and a refractive index detector (RID) in series. The measurements were conducted at 60 °C using DMSO with 0.1 w/v% LiBr as mobile phase at a flow rate of 0.8 mL/min. The calibration was performed with the RID using PMMA standards. For the OL feedstock and modified OL, approx. 3.0 – 4.0 mg was dissolved in 1 mL DMSO. All samples were filtered with a syringe filter (0.45 µm) prior to injection and no aggregation was observed for any sample.

2.3.3. FTIR spectroscopy

The Fourier-transform infrared spectroscopy (FTIR) spectra of the (modified) lignin samples were obtained with a Shimadzu IRSpirit (equipped with an ATR module made from diamond and a KBr window) with 32 cumulative scans and 2 cm^{-1} resolution within 4000 cm^{-1} – 800 cm^{-1}. All spectra were normalized at ≈ 1504 cm^{-1} corresponding with C=C stretching vibrations in aromatics.

2.3.4. ^{1}H-NMR qualitative analysis

^{1}H-NMR spectra were recorded with a Bruker 300 MHz Avance I spectrometer using the zg30 pulse program, 16 scans and a delay time of 1 seconds. The samples (50 – 100 mg) were dissolved in 600 µL DMSO-d_6 and transferred into 5mm NMR tubes.

2.3.5. ^{13}C-NMR qualitative analysis

^{13}C-NMR spectra of lignin samples were recorded on a Bruker 700 MHz Avance II spectrometer at 40 °C equipped with a cryoprobe using inversed gated decoupling and the zgig30 pulse program, 3,000 scans, an acquisition time of 1.5 s and a delay time of 3.0 s. The protocol consisted of dissolving ± 80.0 mg lignin sample in 0.65 mL DMSO-d_6 followed by the addition of ± 2.5 mg relaxation agent $Cr(acac)_3$ and 3.0 – 4.0 mg 1,3,5-trioxane as reference for the chemical shift at 92.9 ppm.

2.3.6. ^{31}P-NMR quantitative analysis

^{31}P-NMR spectra of lignin samples were recorded with a Bruker 400 MHz Avance II spectrometer equipped with a cryoprobe using the zgig pulse program, 32 scans and a delay time of 10 seconds combined with $Cr(acac)_3$ as a relaxation agent, NHND as internal standard and TMDP as phosphorus reagent. The applied ^{31}P-NMR protocol was based on the procedure developed by Argyropoulos with manual phase correction and full auto baseline correction.[54] The spectra are divided into 4 regions corresponding with the internal standard NHND (151.5 – 152.5 ppm), alOHs (145.0 – 150.0 ppm), phOHs (136.5 – 144.5 ppm) and COOHs (133.5 – 136.0 ppm) as can be seen in Figure S3.

2.3.7. Injectability study of gels

The sliding force of the gels were determined with a custom-built syringe holder mounted in the Shimadzu Autograph AGS-X mechanical analyzer equipped with a 5 kN load cell. First, freshly prepared gel solution was transferred into a syringe prior to gelation to avoid trapped air bubbles and obtain a stable packing of the gel in the syringe. A Hamilton 30 cm (G18) metal hub needle was screwed on top of the syringe and mounted into a dedicated aluminum holder. The maximal pressure was set at 5000N to extrude the gel through the syringe tip and needle. The numerical sliding force values were calculated in the linear area (displacement range of 18 – 28 mm).

2.3.8. Rheological study of the self-healing process

Small amplitude oscillatory shear (SAOS) tests were conducted in triplicate with an Anton Paar MCR 702 TwinDrive Modular Compact Rheometer. For that purpose, a parallel plate measuring tool with a diameter of 25 mm was selected. Disk-shaped gel samples with a diameter of 26 mm were prepared 24 hours before the experiments. These disks were loaded on the lower plate, the upper plate was lowered to a trim position of 1.025 mm, and then the sample was carefully trimmed to match the measuring tool diameter in view of finally setting the gap to exactly 1.000 mm. The gel was set to rest for 1 minute to provide temperature stability (set value = 25 °C to avoid solidification of DMSO) and then, extra 10 minutes were provided to allow for a structured rest state formation. After the rest, an amplitude sweep was performed at a constant angular frequency of 1 rad s^{-1} over a shear strain range of 0.01 – 10 %. Immediately afterwards, a time sweep was conducted for 30 minutes (at 1 rad s^{-1}) and a set shear strain of 0.05 %.

3. Results

The results are presented in two main parts, with the first one discussing the effect of the oxyalkylation process (with $GlyCO_3$) with the effect of the work up procedure (*i.e.* precipitation) and the effect of alkalinity and temperature on the OL biopolymer structure followed by the study of the oxyalkylation modification to map the effect of several variables (*i.e.*. catalyst, temperature, time, solvent). In addition, the oxyalkylation

mechanism is elucidated in here. In the 2nd part, boronate ester gels were synthesized with different molar ratios of 1,2-diol and boronate acid functionalities focusing on the potential for self-healing.

3.1. Characterization of beech wood OL feedstock

The OL feedstock was characterized in triplicate (with a 95% confidence interval (C.I.)) with GPC and ^{31}P-NMR. The molecular weight of the highest peak (M_p), weight average molecular weight (M_w) and dispersity (Đ) and numerical values for the concentration of the different OH groups (aliphatic, phenolic and COOH) are shown in Table 1.

Table 1 Properties of beech wood OL feedstock (95% C.I.)

M_p (g mol^{-1})	**M_w (g mol^{-1})**	**Đ**
7,141 ± 29	8,284 ± 85	4.62 ± 0.04
alOH (mmol g^{-1})	**phOH (mmol g^{-1})**	**COOH (mmol g^{-1})**
2.61 ± 0.04	2.43 ± 0.04	0.13 ± 0.01

3.2. Mapping change in OL feedstock characteristics

When handling lignin, it is crucial to consider the complexity of this aromatic biopolymer and the susceptibility of biomass in general to various (undesirable) reactions and structural transformations contingent upon certain environmental conditions (*e.g.* temperature, acidity). In this study, the change of a characteristic (such as the M_w or OH content) was linked to a specific adaptation of a reaction variable in the oxyalkylation. Therefore, it is essential to consider all factors – other than the oxyalkylation reaction variables itself – that cause variations in OL feedstock characteristics.

3.2.1. Effect of the work up procedure

The OL feedstock was dissolved in N,N-dimethylformamide (DMF) at room temperature for 15 minutes by continuous stirring followed by precipitation in a 200 mL 0.01 mol L^{-1} HCl solution and filtration with a Buchner filter to adapt the work up procedure (see Materials & Methods). The M_w value (see Table 2) is slightly higher after the work up (WU) procedure was performed which indicates a structural transformation or more likely loss of low molecular weight lignin fragments/molecules. This hypothesis was further strengthened by the slightly yellowish color of the filtrate (containing the 0.01 mol L^{-1} aqueous HCl solution) after precipitation, caused by low molecular weight lignin fragments that remained in solution. In addition, both molecular weight distributions (MWD) are identical in the high molecular weight region (Figure S4A). Yet, in the low molecular weight region, the MWDs do not exhibit overlap to the same extent. However, after successful oxyalkylation, the low molecular weight molecules will have increased in molar mass and the phOHs will be converted in alOHs, thereby lowering the possibility/occurrence of fractionation (compared to unmodified OL) since the modified lignin will be even less soluble.

Table 2 OL feedstock characterization after performing the work up (WU) procedure and after thermal treatment (for 30 minutes) in DMF in alkaline environment (K_2CO_3) (with 95% C.I.)

Exp	**M_w (g mol^{-1})**	**Đ**	**OH groups (mmol g^{-1})**		
			alOH	**phOH**	**COOH**
OL	8,284 ± 85	4.6	2.61	2.43	0.13
WU	8,555 ± 144	4.2	2.45	2.18	0.11
120°C	10,575 ± 114	4.0	2.25	1.94	0.12
150°C	10,593 ± 177	4.3	2.11	2.07	0.11
175°C	10,328 ± 480	4.6	2.10	2.02	0.11

3.2.2. Effect of the alkalinity and temperature

Since the oxyalkylation was performed at elevated temperatures in presence of base catalysts, it is important to evaluate the effect of the used conditions on the OL feedstock in absence of the oxyalkylation reaction itself. Therefore, the OL was dissolved in DMF as a non-reactive solvent together with 0.1 eq. K_2CO_3 and thermal treatment was conducted for 30 minutes (reflux) at the reaction temperature (120 – 150 °C) and in 1-butylpyrrolidin-2-on (1-BPO, see section 3.6) as a high-boiling non-reactive solvent together with 0.1 eq. K_2CO_3 for 30 minutes at 175 °C. These reaction settings were chosen since the majority of the oxyalkylation experiments throughout this study were performed at these temperatures. Afterwards, the lignin was precipitated and collected as filter residue. The M_w value increased relative to OL feedstock (see Table 2), which initially can be attributed to certain undesirable side reactions. The MWDs in Figure S4B show a loss of molecules in the low molecular weight region while the high molecular weight region changed as well after the thermal treatment in alkaline environment. However, as the Đ did not increase to values higher than 4.6 (= initial Đ), any unwanted polymerization or condensation reactions can be excluded. In addition, both the alOH and phOH content decreased slightly after treatment compared to the OL feedstock.

To conclude, although the M_w and Đ values as well as the OH content is altered by the thermal treatment in presence of K_2CO_3, this degree of change is not necessarily applicable when DMF is replaced by $GlyCO_3$ as solvent. For example, if certain OH functionalities undergo reaction or are eliminated at elevated temperatures, once $GlyCO_3$ is added, these OH groups can directly be modified and thereby preventing any undesirable side reaction taking place. In addition, if certain low molecular weight fragments are lost during the work up procedure, this might be (partially) prevented since the oxyalkylation of OH groups of these low molecular weight fragments increases the M_w, thereby facilitating the precipitation of lignin. Therefore, in the next subsections, all results are compared to the characteristics of the OL feedstock summarized in Table 1 (except explicitly otherwise mentioned in the text).

3.3. Evaluating the effect of catalyst

At first, the oxyalkylation (175 °C – 30 minutes) was carried out in absence of any catalyst (NC). Here, the M_w value (visualized in Figure 3 on the secondary y-axis) was barely affected compared to the OL feedstock. The phOH content (visualized in Figure 3 on the primary y-axis) did not seem to participate in the oxyalkylation since the majority of the phOH groups are still present and the alOH content did not increase.

In fact, the alOH content slightly decreased after reaction which is in accordance with the results of the thermal treatment at 175 °C in DMF. Upon this uncatalyzed reaction, several base catalysts were screened such as DBU as it is often selected as base catalyst to perform the oxyalkylation of different substrates although it is a toxic compound and from a sustainable and green chemistry perspective, should be replaced by a safer alternative.[29], [37], [55] Therefore, K_2CO_3 and KOH were evaluated as well despite their limited solubility in organic solvents, since these compounds are non-toxic and do not contain any critical elements.[56] TBAB, an environmentally friendly phase transfer catalyst,[57] was included in this study as well since it was previously applied in the oxyalkylation of lignins with aliphatic carbonates such as dimethyl carbonate with up to 90% conversion of OH functionalities.[58] The corresponding MWDs are visualized in Figure S5.

The most severe increase in M_w (+ 81%) was obtained with K_2CO_3 while the M_w was minimally affected when TBAB was used (+ 27%). This trend in the M_w values matches the increase in alOH content: while TBAB decreased the alOH content compared to the OL feedstock even though the phOH functionalities partially participated in the modification, the use of K_2CO_3 increased the alOH content with 74%. Both the use of KOH and DBU resulted in a rather similar M_w value and alOH content, both slightly lower than when K_2CO_3 was applied. Kühnel *et al.* determined DBU to be an ideal catalyst to suppress polymerization while catalysts such as K_2CO_3 are prone to catalyze condensation reactions in the oxyalkylation with $PrCO_3$.[33] Their data shows a higher Đ for lignin treated with K_2CO_3 while lignin treated with DBU results in a lower Đ (except when the reaction time was prolonged to 24h) and for 0.5h, the K_2CO_3 and DBU resulted in an M_w of resp. 27,000 and 9,700 g mol^{-1}. However, this phenomenon was not observed here (with $GlyCO_3$) since there is no such substantial difference in M_w values. Moreover, the lignin modified in the presence of K_2CO_3 and having the largest molecular weight is accompanied with the highest alOH content and lowest Đ and thus does not indicate undesirable condensation or polymerization.

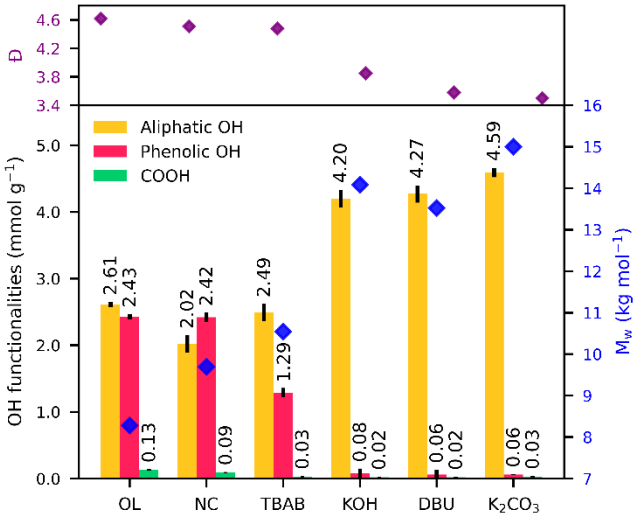

Figure 3 Effect of the catalyst on the oxyalkylation of OL feedstock (at 175 °C for 30 minutes)

The modified lignin samples were evaluated with FTIR as a fast tool to screen the success of the modification reaction (Figure S6). The typical C=C stretching vibrations in aromatics are located at 1600 cm^{-1} and 1510 cm^{-1} and the intensity of the latter signal was normalized for all FTIR spectra. All lignin samples contain sp^3-hybridized C-H bond (methyl and methylene) signals in the range of 2825 cm^{-1} – 3000 cm^{-1} and signals at 1120 cm^{-1}, 1050 cm^{-1} and 1030 cm^{-1} (corresponding with resp. secondary alcohols, C-O alkyl ethers in alkyl aryl ethers and in primary alcohols). The FTIR spectra of the OL feedstock and the oxyalkylated sample obtained after modification without catalyst are very similar. However, when a catalyst was used, a signal was visible at 1050 cm^{-1} indicating successful etherification. Furthermore, the use of K_2CO_3, KOH and DBU resulted in a more distinct signal at 1120 cm^{-1} corresponding with the secondary alcohol in 1,2-diols. Moreover, a strong signal is visible at ≈1790 cm^{-1} in all oxyalkylated samples (though less intense when no catalyst was used) corresponding with the C=O bond in a cyclic carbonate functionality obtained via transesterification (Figure 2). This conclusion is supported by other studies: (1) Kühnel *et al.* attributed this signal to cyclic carbonates obtained via transesterification while signals at 1740 cm^{-1} were attributed to be linear C=O carbonate structures.[29], [33] (2) Duval *et al.* derivatized condensed tannins with $EtCO_3$, $PrCO_3$ and $GlyCO_3$ and observed a C=O signal at wavenumbers < 1750 cm^{-1} for $EtCO_3$ and $PrCO_3$ (= linear carbonates in the modified structure) and at 1786 cm^{-1} for $GlyCO_3$ (= cyclic carbonates in the modified structure by transesterification).[41] In addition, 1,2-diols favor conversion into cyclic carbonates via transesterification with alkali metal salts (such as K_2CO_3 in this study).[37] Furthermore, the undesirable modification/shielding of 1,2-diols into final cyclic carbonate functionalities will be explained more in depth with experimental results in subsection 3.4.2. In conclusion, DBU, KOH and K_2CO_3 perform well though only the latter two can be regarded as sustainable and safe catalysts with the best results in favor of K_2CO_3. Therefore, only K_2CO_3 was taken into consideration in the following subsections/experiments.

3.3.1. Homopolymerization of $GlyCO_3$

Upon the characterization of modified OL with KOH, DBU and K_2CO_3, a viscosity increase was observed of the reaction medium after oxyalkylation. This viscosity increase of $GlyCO_3$ with DBU and K_2CO_3, in absence of lignin, was determined by a plate-and-plate viscometer (Figure S7) with a significant increase at 175 °C (> 15 minutes) when both DBU and K_2CO_3 are applied while no viscosity increase is observable in absence of a catalyst.

To assess whether homopolymerization of $GlyCO_3$ is the cause of this viscosity increase, $GlyCO_3$ as such and after thermal treatment at 175 °C for 30 minutes with K_2CO_3 was analyzed with GPC and ^{1}H-NMR. $GlyCO_3$, prior treatment, is not detectable with the RID of the GPC due to its too low M_w while poly($GlyCO_3$) was detectable due to its larger hydrodynamic volume (*i.e.* M_w) (Figure S8A). In addition, the ^{1}H-NMR spectrum of $GlyCO_3$ clearly distinguishes the different ^{1}H nuclei while after treatment the signals are broadened due to polymerization (Figure

S8B). In conclusion, a more pronounced increase in viscosity caused by homopolymerization occurs when using K_2CO_3, thereby limiting the possible reaction condition settings (*i.e.* reaction temperature and time as discussed in subsection 3.4. and subsection 3.5.). The presence of poly($GlyCO_3$) raises the concern if this homopolymer is present in the collected modified lignin. However, if this would be the case, then a very high OH content would be measured which was not observed and will be further discussed in section 3.4. In addition, for the modified lignin obtained after oxyalkylation with glycerol carbonate at 175 °C for 30 minutes with K_2CO_3, the MWD was determined with two individual detectors, a VWD (280 nm) and RID, similar to the experimental approach of Avérous et al.[32] Since both detector signals result in similar MWDs (see Figure S9) with no extra signals in the RID based MWD, no poly($GlyCO_3$) was present in the collected lignin after performing the oxyalkylation and the work up procedure.

3.4. Mapping the effect of the reaction temperature

Several different reaction temperature ranges for the oxyalkylation with cyclic carbonates are reported in literature which affect the reaction rates and occurrence of side reactions. In this study, three different temperatures (120 – 150 – 175 °C) were experimentally evaluated. All oxyalkylation products (see Figure 4) show an increased M_w value compared to the native OL feedstock (8,300 g mol^{-1}) and which is more pronounced at higher temperatures. Simultaneously, a higher temperature led to a lower Đ value, specifically 4.6 > 4.1 > 3.5. The corresponding MWDs are visualized in Figure S10. A reaction temperature of 200 °C was evaluated as well but resulted in an impossible to collect modified lignin because of a severe increase in viscosity of the reaction mixture due to homopolymerization of $GlyCO_3$.

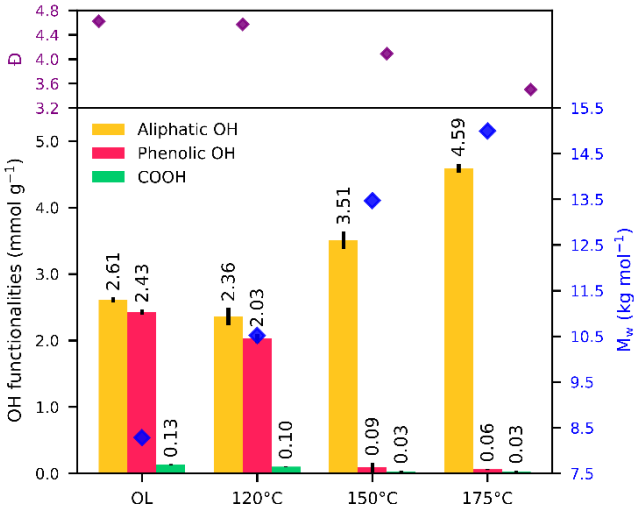

Figure 4 Effect of the reaction temperature on the oxyalkylation of OL feedstock (for 30 minutes with K_2CO_3)

Both the M_w and Đ values of the oxyalkylation product obtained after reaction at 120 °C did not resp. increase and decrease substantially compared to the lignins obtained after reaction at other (higher) reaction temperatures. These results indicate a poor conversion degree which is further supported by the presence of a high residual phOH content (2.03 mmol g^{-1}). Additionally, the alOH content decreased which is possibly caused by structural changes in the OL feedstock due to the elevated reaction temperature which was noticeable as well with the high temperature treatments in DMF (see subsection 3.2.2).

The modified lignins obtained after oxyalkylation at a temperature of 150 °C and 175 °C show complete conversion of the phOH functionalities into 1,2-diols. Remarkably, both the M_w value and alOH content continue to increase with an elevated temperature while complete conversion of phOH and COOH functionalities was already reached with a reaction temperature of 150 °C. This phenomenon was caused by less occurrence of the undesirable internal transesterification at 175 °C (see subsection 3.4.2). The question arises whether the alOH content obtained after lignin treatment at 175 °C is sufficient. Therefore, a formula (Eq. 1) was developed to calculate the theoretical (expected) OH content after oxyalkylation (≈ 6.91 mmol g^{-1}) taking into account several assumptions: **(1)** all OH functionalities are converted into 1,2-diols, **(2)** no side reactions take place, **(3)** both COOHs and phOHs react with $GlyCO_3$ with release of CO_2 and **(4)** the alOH functionalities react with the electrophilic C-atom in the carbonyl bond in the carbonate structure. However, at considered optimal temperature, the highest alOH content is only 4.59 mmol g^{-1} indicating the occurrence of side reactions such as the internal transesterification into cyclic carbonate structures, thereby protecting 1,2-diol functionalities which is described more in depth in subsection 3.4.2.

$$[OH]_{expected} = \frac{[OH]_{i,total} * 2}{1 + [alOH]_i * 0.118 + ([phOH]_i + [COOH]_i) * 0.074}$$

Eq. 1 The expected OH content after oxyalkylation with $GlyCO_3$ when every OH species reacts ($[OH]_{i,\,total}$ the total OH content determined by the sum of alOH, phOH and COOH functionalities; $[alOH]_i$/ $[phOH]_i$/ $[COOH]_i$ the initial OH content of the specific OH functionality; factor 0.118 (= MW of $GlyCO_3$) from the addition of the $GlyCO_3$; factor 0.074 which stands for the addition of $GlyCO_3$ after decarboxylation with release of CO_2 (= 0.044 g/mmol))

To further investigate the oxyalkylated products, ^{13}C-NMR (Figure S11) was applied to gain mechanistic and structural insights. The signals corresponding with the C-atoms C_3 (and C_5) in guaiacyl units (and syringyl units) in the non-etherified aromatics region (142 ppm – 150 ppm) decrease in intensity after oxyalkylation at 150 °C and 175 °C while the signals of these C_3 and C_5-atoms in the etherified aromatics region (150 – 154 ppm) clearly increase. These results support the total conversion of phOH functionalities observed with ^{31}P-NMR at both 150 °C and 175 °C. The raw alOH groups in OL feedstock at 60 ppm show a clear visible signal at 150 °C and 175 °C. Thus, the alOH groups did not fully participate in the oxyalkylation for both temperatures. Kühnel *et al.* published ^{13}C-NMR spectra of oxyalkylated lignin with different cyclic carbonates as reagent. While the raw alOH signal at 60 ppm is barely visible after oxyalkylation with $PrCO_3$ and $BuCO_3$, the signal was

still clearly visible after oxyalkylation with $GlyCO_3$ as well.[29] In another study by Kühnel *et al.*, the authors mention native alOH groups are still present after oxypropylation of OL with similar reaction conditions (*i.e.* 170 °C with both K_2CO_3 and DBU for 0.5 h to 24 h reaction time).[33]

Furthermore, a signal at 154.9 ppm for both oxyalkylated lignin sample spectra is visible corresponding with the cyclic carbonate functionalities (see Figure 2) after partial internal transesterification of the vicinal diols. The FTIR spectra (Figure S12) for both oxyalkylated samples at 150 °C and 175 °C show a distinct signal at 1050 cm^{-1} and at 1120 cm^{-1} from resp. secondary alcohols in 1,2-diols and C-O alkyl ethers in alkyl aryl ethers from the successful oxyalkylation as well as an intense signal corresponding with cyclic carbonate functionalities (1789 cm^{-1}). However, no signal (< 1750 cm^{-1}) could be attributed to aliphatic CO_3 structures (formed by reaction between alOH and $GlyCO_3$). Therefore, the increase in alOH content from 150 °C to 175 °C exists because more cyclic carbonate functionalities are present after reaction at 150 °C, which will be discussed in depth in subsection 3.4.2.

3.4.1. Oxyalkylation with $EtCO_3$

In addition to the oxyalkylation with $GlyCO_3$, a more reactive cyclic carbonate was used as well (*i.e.* 10 eq. $EtCO_3$) and the results are summarized in Table 3. A temperature of 175 °C resulted in a high viscous / solid-like material within the first 10 minutes of reaction which made it impossible to stir the reaction mixture and perform the work up procedure. Therefore, only a temperature of 120 °C and 150 °C is reported with $EtCO_3$ in here. After reaction at 120 °C, not all phOH groups were converted while at 150 °C, all phOH groups were converted and a high alOH content was obtained which was accompanied by a very high M_w value of ≈ 29,200 g mol^{-1}. Even after reaction at 120 °C, the M_w was already high with a value of ≈ 12,500 g mol^{-1}. However, it is important to take into account that the highest molecular weight fragments are exceeding the highest M_w value in the calibration range. Therefore, the M_p value is more accurate to use in these experiments (with M_p within the calibration range) with values of ≈ 12,250 and ≈ 26,200 g mol^{-1} for products obtained after resp. 120 °C and 150 °C. These high molecular weight values could be the result of side reactions such as chain extension (= grafting from polymerization of $GlyCO_3$ from lignin) and crosslinking [35], [39] but would inherently lead to a final low OH content because during crosslinking, OH functionalities are consumed (see Figure 2) while during chain extension, the amount of OH groups would remain the same, yet the molar mass will increase, hence a decrease in OH content (mmol g^{-1}) would be observed. However, the theoretical OH content after oxyalkylation (3.86 mmol g^{-1}), see Eq. 2, is close to the experimentally obtained OH content of ≈ 3.76 mmol g^{-1} after reaction at 150 °C. Thus, indicating (1) low amount of undesirable reactions that affect the OH content and (2) conversion of native alOH into extended primary alOH functionalities.

$$[OH]_{expected} = \frac{[OH]_{i,total}}{1 + [alOH]_i * 0.088 + ([phOH]_i + [COOH]_i) * 0.044}$$

Eq. 2: The expected OH content after oxyalkylation with $EtCO_3$ when every OH species reacts ($[OH]_{i,\ total}$ the total OH content determined by the sum of alOH, phOH and COOH functionalities; $[alOH]_i$/ $[phOH]_i$/ $[COOH]_i$ the initial OH content of the specific OH functionality; factor 0.088 (= MW of $EtCO_3$) from the addition of the $EtCO_3$; factor 0.044 which stands for the addition of $EtCO_3$ after decarboxylation with release of CO_2 (= 0.044 g/mmol))

The latter conclusion is supported by the fact that if the alOH groups are not converted by $EtCO_3$, then the total amount of moles of OH groups (numerator) does not change yet the formula (Eq. 3) is altered in the denominator and a much higher theoretical OH content would be obtained of ≈ 4.65 mmol g^{-1}.

$$[OH]_{expected} = \frac{[OH]_{i,total}}{1 + ([phOH]_i + [COOH]_i) * 0.044}$$

Eq. 3: The expected OH content after oxyalkylation with $EtCO_3$ when alOH do not react ([OH]i, total the total OH content determined by the sum of alOH, phOH and COOH functionalities; [phOH]i/ [COOH]i the initial OH content of the specific OH functionality; factor 0.044 which stands for the addition of $EtCO_3$ after decarboxylation with release of CO_2)

The M_w values obtained after modification with $EtCO_3$ are much higher than after modification with $GlyCO_3$ which is contradictory since a higher molecular weight extension fragment is added to lignin after modification with $GlyCO_3$. Thus, it is likely that the modified lignin with $GlyCO_3$ should have a higher M_w value. The low experimentally obtained M_w values indicate limited conversion of native alOH groups which is supported by the ^{13}C-NMR spectra described earlier. The FTIR spectra (Figure S13) of the modified lignin with $EtCO_3$ show no signal at 1790 cm^{-1} since formation of final cyclic carbonate functionalities via internal transesterification can only occur with $GlyCO_3$. However, a signal at 1740 cm^{-1} is present after treatment with $EtCO_3$ at 150 °C corresponding with aliphatic carbonate groups,[41] thereby indicating the reaction between alOH and $EtCO_3$ takes place. This signal is never visible when $GlyCO_3$ was used, which supports the hypothesis that the alOH groups barely react with $GlyCO_3$ resulting in no formation of aliphatic CO_3 functionalities and no chain extension of 118 g mol^{-1}. Several studies discuss the formation of ethers and linear carbonates after oxyalkylation between alOH and cyclic carbonates.[29], [35] However, since it is established here that alOH of the investigated lignin react with $EtCO_3$ with a visible signal of linear carbonates (even after reaction at 120 °C), it can be concluded that once alOH react, they form linear carbonates (possibly in combination with the formation of ethers).[7], [39]

Table 3 Effect of reaction temperature on the oxyalkylation of OL feedstock with $EtCO_3$ (for 30 minutes with K_2CO_3)

T	M_w (g mol^{-1})		OH content (mmol g^{-1})		
(°C)	M_p	M_w	alOH	phOH	COOH
120	12,250	12,500	2.68	1.75	0.02
150	26,200	29,200	3.76	0.07	0.03

3.4.2. Hydrolysis of the cyclic carbonate functionalities

In the previous subsections, the presence of cyclic carbonate functionalities after oxyalkylation with $GlyCO_3$ was proven with FTIR while no linear carbonates were observed as proven by the absence of a signal at ≈ 1740 cm^{-1}. The hydrolysis of these cyclic carbonate functionalities (see Figure 5) was conducted and the alOH content was determined before and after hydrolysis in order to determine the concentration of the

cyclic carbonate functionalities (= Δ[alOH]/2). The modified lignins (after oxyalkylation with 10 eq. $GlyCO_3$ and 0.1 eq. K_2CO_3 for 30 minutes at both 150 °C and 175 °C) were exposed to a 0.2M KOH in ethanol solution for 15 minutes (reflux). The hydrolysis of both samples was successful since the signal at ≈ 1790 cm^{-1} in the FTIR spectra (Figure S14) is barely visible anymore. Specifically for the oxyalkylated lignin at 175 °C, the alOH content increased after hydrolysis (Table 4) to ≈ 5.44 mmol g^{-1}, thus, ≈ 0.42 mmol g^{-1} cyclic carbonate functionalities were present after oxyalkylation, thereby protecting ≈ 0.84 mmol g^{-1} of alOH groups. However, the theoretical OH content of ≈ 6.91 mmol g^{-1} – described in subsection 3.4 – was not yet met due to (1) the limited reactivity of the alOH functionalities with $GlyCO_3$ and (2) possibly other reactions upon the internal transesterification into cyclic carbonate functionalities which are difficult to detect.

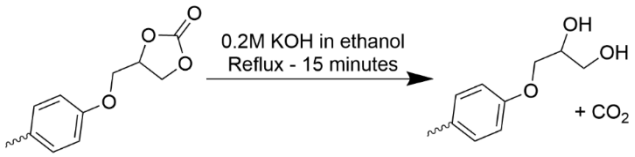

Figure 5 Hydrolysis of cyclic carbonate functionalities

As described in subsection 3.4, the alOH content increased when the reaction temperature was elevated from 150 °C to 175 °C which was attributed to the dominance of an undesirable reaction at 150 °C. Since it was determined that alOHs take at most slightly part in the reaction (FTIR and ^{13}C-NMR data and the comparison with the theoretical OH content), the only explanation for this increase is, indeed, that a much higher cyclic carbonate content after oxyalkylation at 150 °C should be present whereby a high number of diols are shielded. The alOH content after hydrolysis is about 5.39 mmol g^{-1} which implies approx. 0.94 mmol g^{-1} cyclic CO_3 functionalities are present after oxyalkylation at 150 °C (which is approx. twice as much as after oxyalkylation at 175 °C). This phenomenon might occur because at higher temperatures, the homopolymerization of $GlyCO_3$ occurs more thereby competing with the internal transesterification to cyclic carbonates or at higher temperatures, cyclic carbonates might be more prone to undergo thermal cleavage. In conclusion, the undesirable internal transesterification products are more dominant at 150 °C resulting in the shielding of a high amount of alOH functionalities. Therefore, it is important to perform the reaction at 175 °C to minimize the formation of undesirable functionalities while sufficiently suppressing the homopolymerization of $GlyCO_3$.

Table 4 OH content before and after hydrolysis of oxyalkylated OL and cyclic CO_3 content in oxyalkylated lignin

T (°C)	OH content (mmol g^{-1})		
	After oxyalkylation	**After hydrolysis**	**Cyclic CO_3 content**
150	3.51	5.39	ca. 0.94
175	4.59	5.44	ca. 0.42

3.5. Mapping the reaction time effect

3.5.1. Oxyalkylation at 150 °C

In the previous subsection, the combination of 150 °C and 30 minutes resulted in complete conversion of phOH and COOH functionalities. However, the increase in alOH content was more pronounced at 175 °C because of the reduced occurrence of the undesirable internal transesterification leading to shielding of 1,2-diols. However, varying the reaction time at 150 °C might still increase the alOH content substantially while avoiding the necessity to perform the modification at 175 °C. If the reaction time at 150 °C was only 15 minutes, residual phOH functionalities were present (Figure 6), as expected, while the M_w value increased with approx. 47% compared to the OL feedstock. Increasing the reaction time to 30 minutes slightly increased the alOH content in combination with a further increase in M_w and complete conversion of phOH and COOH functionalities. Increasing the reaction time by a factor of 2 from 30 to 60 minutes only slightly increased both the M_w value and alOH content. In conclusion, the alOH content of all obtained samples after oxyalkylation at 150 °C with varying reaction times is substantially lower than the alOH content obtained after treatment of OL feedstock at 175 °C for 30 minutes (≈ 4.59 mmol g^{-1}). Furthermore, the Đ was higher for all samples treated at 150 °C (4.0, 4.1, 4.0 for resp. 15 min, 30 min and 60 min) compared to the modified lignin sample obtained after 30 minutes at 175 °C reaction (3.5). The corresponding MWDs are visualized in Figure S15.

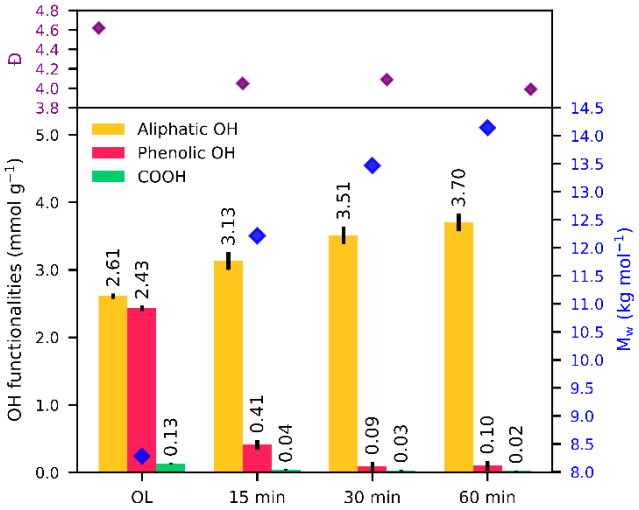

Figure 6 Effect of the reaction time on the oxyalkylation of OL feedstock (at 150 °C with K_2CO_3)

3.5.2. Oxyalkylation at 175 °C

The reaction time was varied (5 min – 15 min – 30 min – 60 min) at the most optimal temperature (*i.e.* 175 °C) in Figure 7. Similar to the oxyalkylation at 150 °C, an increased reaction time (60 minutes) results in a higher M_w value up to 17,830 g mol^{-1} and a lower Đ (resp. 3.9; 3.7; 3.5; 3.3 with increasing reaction time). At 175 °C, the reaction time could be reduced to 5 minutes while almost all phOH groups took part in the oxyalkylation. A reaction time of 60 minutes increased the alOH content up to 5.02 mmol g^{-1}, however the solid sample could not be completely recovered from the flask since the modified lignin was difficult to precipitate and afterwards filtered properly. Therefore, the reaction at 175 °C for 60 minutes resulted in severe loss of lignin and was not considered in further experiments in this study. To illustrate this phenomenon, the oxyalkylation (= homopolymerization) of $GlyCO_3$ was performed in absence of lignin and the viscosity was measured. The viscosity of the reaction mixture (without lignin) increased from 56.71 ± 0.70 mPa.s prior applying heat up to 26,906 ± 1,302 mPa.s (after 1h) as visualized in Figure S7. This indicates the encountered difficulty during the work up procedure when a long reaction time is applied for the oxyalkylation. The corresponding MWDs are visualized in Figure S16.

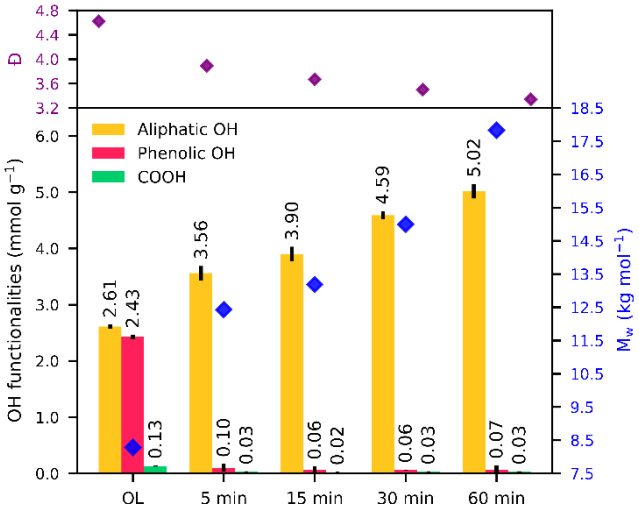

Figure 7 Effect of the reaction time on the oxyalkylation of OL feedstock (at 175 °C with K_2CO_3)

Upon the numerical values obtained from ^{31}P-NMR, the different spectra are visualized in Figure S17. When a 1,2-diol is formed, four different signals can be observed.[29], [41] Those four signals are in pairs at 146.0 – 146.8 ppm and 146.8 – 148.0 ppm corresponding to resp. secondary and primary alcohols. With an increasing reaction time (and thus an increased OH content), the signal intensity at 146.2 ppm increases. After 60 minutes reaction, in the spectrum, four clearly distinguished signals with high intensity can be seen accompanied with a high OH content (≈ 5.02 mmol g^{-1}). However, taking into consideration the challenging work up procedure with limited amount of collected sample, a reaction time of 30 minutes was chosen as optimal to continue in this work.

3.6. Evaluating an additional solvent in the oxyalkylation

In previous experiments, the $GlyCO_3$ acted as reagent as well as solvent which limited the reaction temperature and time as an increase in viscosity adversely impacted the work up procedure. Vieira *et al.* detected similar observations in viscosity with $PrCO_3$ and subsequently mapped the interactions of the process variables on the viscosity.[34] Thereby, an additional solvent could reduce the viscosity – by dilution – at elevated temperatures while it is still possible to perform the work up procedure. A limited amount of published research did investigate the addition of a solvent such as DMF in the oxyalkylation with $EtCO_3$ by Kao *et al.*[59] and dimethyl sulfoxide (DMSO) in the oxyalkylation of xylan with $PrCO_3$ by Akil *et al.*[55], [60] However, those solvents lack safety and sustainability implementation strategies. Avérous et al. took a different approach by ethoxylating in polyethylene glycol to circumvent a multiple-step process to obtain a liquid polyol mixture that can

entirely be applied in polyurethane resin thermal insulation foams.[61] In this study, 1-BPO was used since it is a green solvent with a high boiling point of 243.8 °C and 1-BPO does not contain hydroxyl (or amine) groups which can take part in the oxyalkylation with glycerol carbonate. Moreover, to the best of our knowledge, no ring-opening of 1-BPO with alcohols can occur at the investigated reaction conditions.[62]

In a first step, the oxyalkylation was performed at 175 °C (30 minutes – K_2CO_3) in presence of either DMSO or 1-BPO with varying lignin/solvent weight ratios (resp. 0.50 and 0.20) to study the effect of dilution. The addition of DMSO was evaluated solely because lignin dissolves very well in this aprotic solvent. It was immediately noticeable that OL started to dissolve at room temperature in the extra solvents. Both DMSO (1.0 g and 2.5 g) and 1-BPO (1.0 g and 2.5 g) resulted in roughly similar alOH contents (Figure S18) compared to the experiment at 175 °C without additional solvent and similar MWDs were obtained for all experiments performed in presence of solvent at 175 °C (Figure S19). For all four samples, the carbonate signal at 1790 cm^{-1} was present (Figure S20) and thus the dilution of the reaction mixture could not inhibit the transesterification into the cyclic carbonate functionalities.

The 2nd step involved the use of solely 1-BPO in the oxyalkylation at 200 °C to evaluate whether this high temperature is beneficial for the overall OH conversion. DMSO was not exposed to temperatures > 175 °C due to the boiling point of 189 °C. After reaction, the filter residue was very difficult to remove from the filter paper. Therefore, a filter crucible (= sintered glass with a pore diameter range of 10 µm – 16 µm) was used to easily recover the precipitated lignin after oxyalkylation at 200 °C. The obtained lignin showed, for both 1.0 g and 2.5 g 1-BPO, complete conversion of phOH and COOH functionalities though the alOH content is low (< 3.00 mmol g^{-1}) as can be seen in Figure S18. Moreover, the M_w value increased severely after a 200 °C treatment which might be due to condensation/crosslinking (see Figure S19) that drastically alters the lignin structure with Đ values of ≈ 4.5 (still more narrowly distributed than OL). It is likely that structural changes occurred since the OL feedstock was pulped at 170 °C from beech wood, thereby a temperature exceeding the pulping temperature might even depolymerize certain easy-to-cleave ether bonds (*e.g.* *β*-O-4) followed by condensation of unstable and reactive intermediates. In addition, the cyclic carbonate signal at 1790 cm^{-1} is completely absent (Figure S21) which might be due to stability issues (= decomposition) at 200 °C (which is likely given the temperature dependence of the presence of cyclic carbonate functionalities as determined in subsection 3.4.2). Kim *et al*. reported an elevated temperature increases the weight loss of lignin and resp. increases and decreases the carbon and oxygen content.[63] Furthermore, even cleaving certain *β*-O-4 bonds solely by heat treatment is possible, starting from 250 °C, while lower temperatures can achieve cleavage of methoxy groups and propyl side chains.[63] All this literature of the temperature sensitivity of lignin is in correspondence with the results obtained in subsection 3.2.2 (taking into account the effect of alkalinity as well).

3.7. Greenness evaluation by the CHEM21 Metrics Toolkit

The modification and implementation of lignins is important for increasing the bio-based content of applications and consumer products. However, the path taken during this modification and/or implementation should be taken into account as well. In this research, an adaptation of the CHEM21 Metrics Toolkit was used to assess greenness of the proposed modification protocol (Table 5) which was proposed by Jacobs *et al*.[7]

The excess amount of cyclic carbonate, *i.e.* 10 eq. as applied in this study, results in a red flag, although 10 eq. was evaluated as a minimum amount to ensure all lignin was dissolved and the reaction mixture was thoroughly stirred. In this study, the excess of $GlyCO_3$ was not recycled since it was lost during the precipitation step. However, even if the $GlyCO_3$ is isolated after reaction, due to homopolymerization it is less valuable to use in further experiments. In addition, it is important to note that an additional solvent would increase the complexity of the reaction mixture and often leads to suboptimal alternatives when looking into green and renewable solvents. Moreover, due to the complexity of lignin with a wide variety of functionalities, the possibility of lignin-solvent interactions/reactivity should be taken into consideration as well. The cyclic carbonates are regarded as green solvents by the CHEM21 Toolkit and are potentially bio-based.[7] For example, $GlyCO_3$ can be made by reaction between glycerol and CO_2 or a dialkyl carbonate or urea.[30], [36], [64]

The catalyst cell is colored amber since K_2CO_3 is a non-recyclable catalyst though no critical elements are involved. The temperature/energy cell is flagged red since a high temperature is necessary for the oxyalkylation – and to inhibit the internal transesterification – and is thereby more energy intense. However, energy is not solely dependent on the temperature since the reaction time is a crucial factor for the energy demand as well. While often long reaction times (> 1h) are described in literature,[37], [38] this research has found a reaction time of 30 minutes (at 175 °C) to be sufficient and optimal to convert all phOH and COOH functionalities and to obtain a maximal alOH content. However, the CHEM21 metrics toolkit adaptation does not take into account the reaction time but solely the required temperature.

The modification is carried out in batch, which is mainly due to the difficult solubility behavior of lignin at room temperature in a wide range of solvents. While a continuous reaction would be beneficial in terms of energy management and minimizing solvent consumption, no continuous process has been reported for the modification of lignin (besides several depolymerization strategies).[7]

3.8. Developing a boronate ester gel

Boronate ester gels were developed by dissolving both oxyalkylated lignin and benzene-1,4-diboronic acid (B^0) into DMSO followed by the addition of an aqueous NaOH solution to obtain tetragonal boronate anions (B^-) resulting in the formation of 5-ring dioxaborolanes (B^-L) as visualized in Figure 8.[47], [49] The amount of crosslinker was determined based on the 1,2-diol content which was assumed to be [1,2-diol] = ($[alOH]_{after\ oxyalkylation}$ - $[alOH]_{initial}$)/2 = 0.99 mmol g^{-1} since it was determined that native alOH functionalities do not participate in the oxyalkylation reaction.

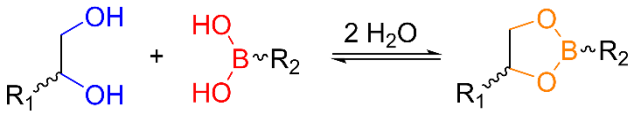

Figure 8 Dioxaborolane formation between a 1,2-diol and boronic acid functionality

As a proof-of-concept (PoC), both unmodified OL feedstock (properties see Table 1) and oxyalkylated lignin were evaluated as starting material in the synthesis of boronate ester gels by dissolving 0.2 g (modified) lignin with an appropriate amount of benzene-1,4-diboronic acid (which corresponds to a 1:1.15 molar ratio diol : boronic acid functionalities) in 1.00 mL DMSO. Next, 1 mL of 1M NaOH was added and the mixture was thoroughly stirred for 2 minutes. For the OL feedstock, no gelation occurred which was observed when the glass recipient was rotated 180° (see Figure 9A). OL feedstock does not contain 1,2-diols, thereby no dioxaborolanes can be formed. In case of the modified OL substrate, gelation was observed and all DMSO and water (total of 2 mL) were retained in the gel structure. In this case, an equilibrium (K_{eq}) occurred (Figure 8) whereby bonds split and form continuously.[44]

Table 5 Greenness evaluation by an adaptation of the CHEM21 Metrics Toolkit

Stoichiometric (S) or excess (E)	Solvents/reagents	Catalyst	Critical Elements	Temperature/energy (°C)	Batch (B)/ Continuous (C)
E	Glycerol carbonate ($GlyCO_3$)	K_2CO_3	-	175	B

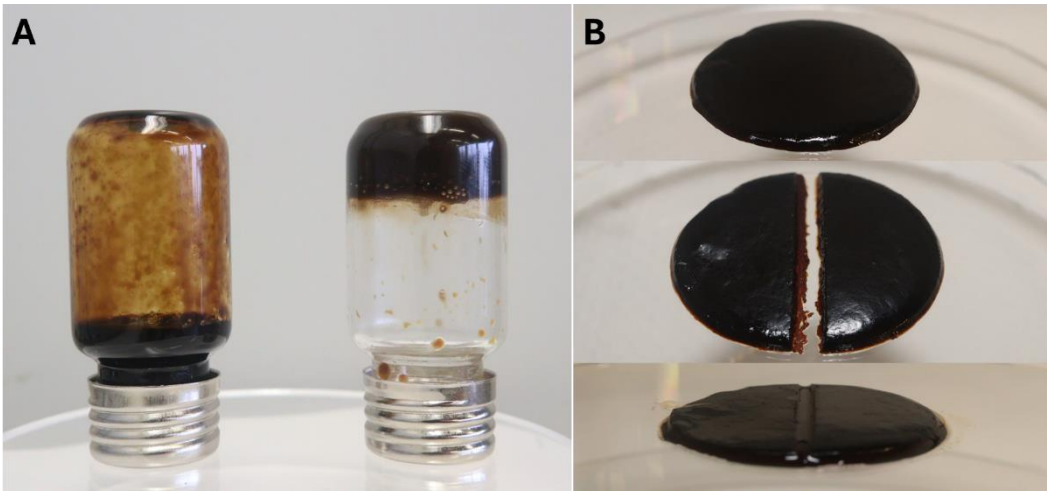

Figure 9 Boronate ester synthesis (**A**) with no gelation when OL feedstock was applied and gelation with modified OL (after oxyalkylation with 10 eq. $GlyCO_3$ and 0.1 eq. K_2CO_3 for 30 minutes at 175 °C) and self-healing phenomenon (**B**) of a cut in the preformed disk-shaped gel (with 1:1.15 mole ratio)

3.8.1. Effect of lignin/crosslinker ratio

To study the effect of the lignin/crosslinker ratio, several gels were successfully synthesized by adding different amounts of benzene-1,4-diboronic acid (as crosslinker) with a 1:1.15 molar ratio, a 1:2.30 molar ratio and a 1:4.60 molar ratio of functionalities (*i.e.* 1,2-diols : boronic acids). It is noteworthy that in the 1:4.60 ratio case the excess of crosslinker did not result in a crosslinked gel but remained a liquid. The gels were characterized by measuring the sliding force by extruding the gels through a needle and by rheology with pre-shaped disk-like lignin-based gel samples.

The sliding force values (Figure S22) reveal that a 4.60 times excess of boronic acid functionalities compared to 1,2-diol groups result in a low linear sliding force profile (6.5 ± 0.5 N) since all diol functionalities are capped by the excess of crosslinker and thereby no crosslinking occurred. Adding less crosslinker resulted in a higher sliding force (33.5 ± 14.8 N) as more crosslinking can occur. Adding only 1.15 times the amount of boronic acid functionalities compared to 1,2-diols results in the highest sliding force to extrude the gel material (64.1 ± 9.2 N) through the syringe and needle and indicates the highest crosslink density of all three experiments. The lowest crosslink ratio applied in this study can theoretically result in maximum crosslinking. The linear region in the sliding force evolution was chosen to be in between 18 mm and 28 mm displacement since the initial peaks in the first 8 to 16 minutes were the result of air bubbles trapped in the bottom of the syringe during loading of the syringe with liquid mixture prior to curing.

Small amplitude oscillatory shear (SAOS) tests were conducted to support the results obtained with the sliding force measurement. Previous experiences showed that the gel could not be first manufactured and then scooped directly on the measuring tool. This method showed low reproducibility, thus we had to premanufacture disk-shaped gel samples. During the screening phase, we observed that the disk shapes needed a rest time of at least 10 minutes (see Figure 10 for the overview of one full sample measurement). This time was necessary for the internal molecular structure of the gel to be at rest state, which is the objective of any SAOS rheology measurement. Next, the disk-shaped gels underwent an amplitude sweep. For both the 1:2.30 and 1:1.15 ratios, the storage modulus (G') is larger than the loss modulus (G"), indicating a viscoelastic material with predominating elastic behavior, as can be linked to the crosslinked nature of the system. The gel with the least amount of crosslinker (1:1.15) resulted in the highest storage and loss moduli, related to the increased crosslink density.[65] These results support the trend in sliding force.

Each amplitude sweep ended in the non-linear viscoelastic region (NLVR) with the inherent intention to destruct the inner molecular structure of the sample and then, a time sweep was conducted to evaluate if self-healing was occurring at 0.05% shear strain (well within the LVR as can be seen in Figure S23):

1) The gels with a 1:2.30 functionality ratio show a self-healing behavior with a gradual increase of the storage and loss moduli especially within the first 10 minutes. After 10 minutes, the values reach a steady-state which is lower than the original storage and loss moduli before destruction, thereby indicating only partial restoration of the gels.
2) The gels with a 1:1.15 functionality ratio show some self-healing within the first 10 minutes as well but more importantly, these gels show almost instantly storage and loss moduli similar to those before destruction (namely, the values of the sample at the LVR). In Figure 9B, a visual cut was made of the disk-shaped sample and after 1h the cut was already partially healed from a visual observation.

Hence, the gels with a 1:2.30 ratio of chemical functionalities (1,2-diol : boronic acid) are susceptible to destruction with only partial self-healing behavior, while the gels with limited a 1:15 ratio of chemical functionalities (1,2-diol : boronic acid) are able to restore the intrinsic molecular structure completely.

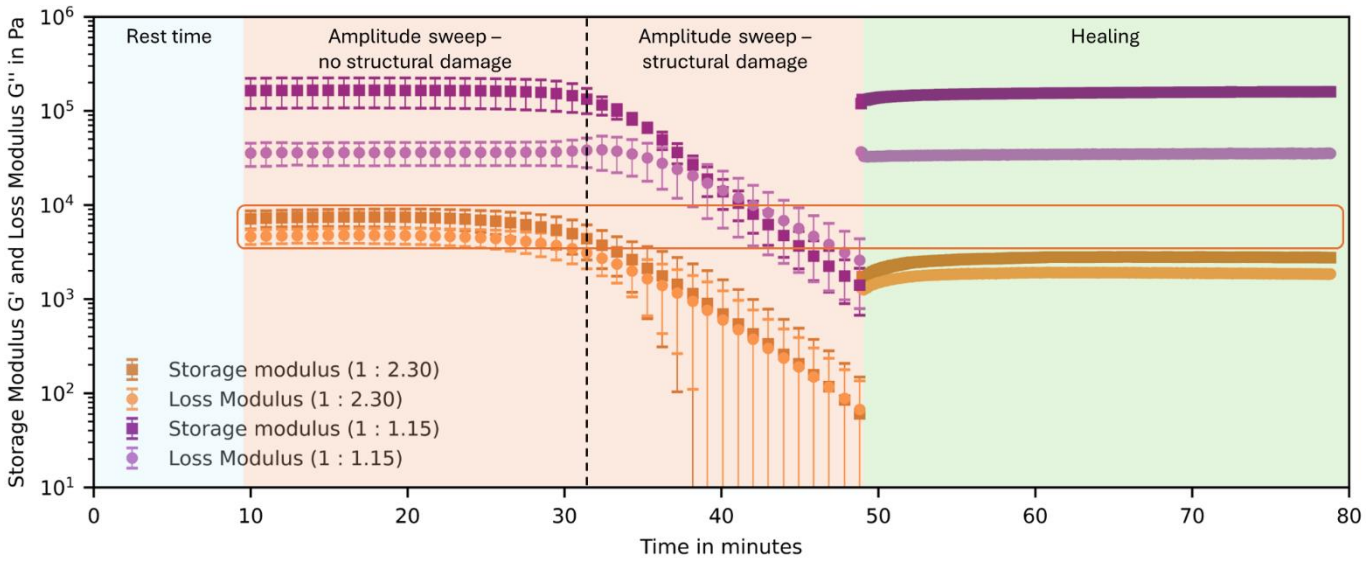

Figure 10 Oscillatory rheology with (left – orange background) oscillatory amplitude sweeps (0.01 – 10 % strain) at 1 rad s^{-1} and (right – green background) oscillatory time sweeps for 30 minutes at 1 rad s^{-1} with 0.05% shear strain in the linear viscoelastic region

4. Conclusion

In this research, beech wood OL feedstock was successfully modified with $GlyCO_3$ into a polyol with a uniform functionality (*i.e.* alOH groups), thereby, exploring the possibilities to use lignin as a valuable building block in thermosets such as polyesters and polyurethanes. Several base catalysts were evaluated whereby both DBU and K_2CO_3 were amongst the top performing ones. However, the K_2CO_3 catalyst results in both a higher M_w value and higher final alOH content than DBU, making it the most efficient and sustainable one. Additionally, it was determined that the native alOH functionalities barely react with $GlyCO_3$ and that an internal transesterification occurred for all reaction conditions resulting in shielding of 1,2-diols. Moreover, a high temperature (175 °C) inhibited the formation of cyclic carbonate functionalities whereby a smaller amount of 1,2-diols was shielded. Thereby, this study contributes to the literature to demystify the mechanism and the occurrence of undesirable reactions in the oxyalkylation with $GlyCO_3$. Furthermore, the effect of the reaction temperature was mapped whereby the highest alOH content was obtained at 175 °C while lower temperatures were disadvantageously affected by lower phOH conversions and/or more shielding of 1,2-diols. Higher temperatures resulted in difficulties in the work up procedure due to polymerization of $GlyCO_3$. In order to circumvent this challenge, an extra solvent (1-BPO) was added to the reaction mixture in order to dilute and reduce the final viscosity. However, a temperature of 200 °C with 1-BPO disrupted the conversion degrees and resulted in a poor final alOH content due to condensation/repolymerization (severe increase in M_w). An optimal set of reaction conditions (175 °C – 30 minutes – 0.1 eq. K_2CO_3 – 10 eq. $GlyCO_3$) managed to produce an oxyalkylated sample with an alOH content of 4.59 mmol g^{-1} and which did not contain any poly($GlyCO_3$). However, even after hydrolyzing the final cyclic carbonate structures and thereby further increasing the alOH content to 5.44 mmol g^{-1}, the theoretically calculated alOH content of 6.91 mmol g^{-1} was not yet achieved. This further supports the non-reactivity of the native alOH groups with $GlyCO_3$. The oxyalkylation at optimal conditions was sufficient to synthesize preliminary gels by crosslinking the obtained vicinal diols in lignin with benzene-1,4-diboronic acid. Especially with the 1:1.15 molar ratio of chemical functionalities (1,2-diol : boronic acid), a gel was made which obtained immediately after destruction shear storage and loss moduli similar to the values before destruction. Thus, this study demonstrated the successful design and use of bio-polyols obtained through the green oxyalkylation of organosolv lignin for making self-healing boronate ester gels. The formation of a gel structure is part of future biobased hydrogel development with self-healing properties at physiological pH.

5. Statements & declarations

B.J. and S.D. both acknowledge the Research Foundation Flanders (FWO) for financial support through grant 1S75824N and 1S19025N, respectively. We thank the NMR Expertise Centre (Ghent University) for providing support and access to its NMR infrastructure.

6. Data availability

Data will be made available on request.

7. References

[1] B. Zhang, G. Qiang, K. Barta, and Z. Sun, "Bio–based polymers from lignin," *Innov. Mater.*, vol. 2, no. 2, p. 100062, 2024, doi: 10.59717/j.xinn-mater.2024.100062.

[2] L. Yang *et al*., "Shifting from fossil-based economy to bio-based economy: Status quo, challenges, and prospects," *Energy*, vol. 228, p. 120533, 2021, doi: https://doi.org/10.1016/j.energy.2021.120533.

[3] C. Okkerse and H. van Bekkum, "From fossil to green," *Green Chem.*, vol. 1, no. 2, pp. 107–114, 1999, doi: 10.1039/A809539F.

[4] J. Lauwaert *et al.*, "Pilot scale recovery of lignin from black liquor and advanced characterization of the final product," *Sep. Purif. Technol.*, vol. 221, pp. 226–235, 2019, doi: https://doi.org/10.1016/j.seppur.2019.03.081.

[5] M. Fache, B. Boutevin, and S. Caillol, "Vanillin Production from Lignin and Its Use as a Renewable Chemical," *ACS Sustain. Chem. Eng.*, vol. 4, no. 1, pp. 35–46, Jan. 2016, doi: 10.1021/acssuschemeng.5b01344.

[6] P. Buono, A. Duval, L. Avérous, and Y. Habibi, "Clicking Biobased Polyphenols: A Sustainable Platform for Aromatic Polymeric Materials," *ChemSusChem*, vol. 11, no. 15, pp. 2472–2491, Aug. 2018, doi: https://doi.org/10.1002/cssc.201800595.

[7] B. Jacobs *et al.*, "Sustainable lignin modifications and processing methods - green chemistry as the way forward," *Green Chem.*, vol. 25, pp. 2042–2086, 2023, doi: 10.1039/D2GC04699G.

[8] A. El Bouhali, P. Gnanasekar, and Y. Habibi, "Chapter 5 - Chemical modifications of lignin," H. Santos and P. B. T.-L.-B. M. for B. A. Figueiredo, Eds., Elsevier, 2021, pp. 159–194. doi: https://doi.org/10.1016/B978-0-12-820303-3.00012-6.

[9] E. S. Esakkimuthu, D. DeVallance, I. Pylypchuk, A. Moreno, and M. H. Sipponen, "Multifunctional lignin-poly (lactic acid) biocomposites for packaging applications ," *Frontiers in Bioengineering and Biotechnology* , vol. 10. 2022. [Online]. Available: https://www.frontiersin.org/articles/10.3389/fbioe.2022.1025076

[10] A. Nasrullah, A. H. Bhat, A. Sada Khan, and H. Ajab, "9 - Comprehensive approach on the structure, production, processing, and application of lignin," in *Woodhead Publishing Series in Composites Science and Engineering*, M. Jawaid, P. Md Tahir, and N. B. T.-L. F. and B.-B. C. M. Saba, Eds., Woodhead Publishing, 2017, pp. 165–178. doi: https://doi.org/10.1016/B978-0-08-100959-8.00009-3.

[11] S. Constant *et al.*, "New insights into the structure and composition of technical lignins: a comparative characterisation study," *Green Chem.*, vol. 18, no. 9, pp. 2651–2665, 2016, doi: 10.1039/C5GC03043A.

[12] Bioenergy Technologies Office, "Cellulosic Sugar and Lignin Production Capabilities RFI Responses," 2019. https://www.energy.gov/eere/bioenergy/cellulosic-sugar-and-lignin-production-capabilities-rfi-responses (accessed May 16, 2023).

[13] G. Tofani, E. Jasiukaitytė-Grojzdek, M. Grilc, and B. Likozar, "Organosolv biorefinery: resource-based process optimisation, pilot technology scale-up and economics," *Green Chem.*, vol. 26, no. 1, pp. 186–201, 2024, doi: 10.1039/D3GC03274D.

[14] J.-L. Wertz, M. Deleu, S. Coppée, and A. Richel, *Hemicelluloses and Lignin in Biorefineries*. CRC Press, 2017. doi: 10.1201/b22136.

[15] N. Brosse, M. H. Hussin, and A. A. Rahim, "Organosolv Processes BT - Biorefineries," K. Wagemann and N. Tippkötter, Eds., Cham: Springer International Publishing, 2019, pp. 153–176. doi: 10.1007/10_2016_61.

[16] Fraunhofer, "Lignocellulose biorefinery," 2023. https://www.cbp.fraunhofer.de/en/range-of-services/processing-of-raw-materials/lignocellulose-biorefinery.html

[17] Y. Ge and Z. Li, "Application of Lignin and Its Derivatives in Adsorption of Heavy Metal Ions in Water: A Review," *ACS Sustain. Chem. Eng.*, vol. 6, no. 5, pp. 7181–7192, May 2018, doi: 10.1021/acssuschemeng.8b01345.

[18] A. Boarino and H.-A. Klok, "Opportunities and Challenges for Lignin Valorization in Food Packaging, Antimicrobial, and Agricultural Applications," *Biomacromolecules*, vol. 24, no. 3, pp. 1065–1077, Mar. 2023, doi: 10.1021/acs.biomac.2c01385.

[19] B. M. Upton and A. M. Kasko, "Strategies for the Conversion of Lignin to High-Value Polymeric Materials: Review and Perspective," *Chem. Rev.*, vol. 116, no. 4, pp. 2275–2306, Feb. 2016, doi: 10.1021/acs.chemrev.5b00345.

[20] S. Gonçalves, J. Ferra, N. Paiva, J. Martins, L. H. Carvalho, and F. D. Magalhães, "Lignosulphonates as an Alternative to Non-Renewable Binders in Wood-Based Materials," *Polymers*, vol. 13, no. 23. 2021. doi: 10.3390/polym13234196.

[21] "Has lignin's time finally come?," *C&EN Glob. Enterp.*, vol. 94, no. 39, pp. 35–37, Oct. 2016, doi: 10.1021/cen-09439-bus2.

[22] L. Dessbesell, M. Paleologou, M. Leitch, R. Pulkki, and C. (Charles) Xu, "Global lignin supply overview and kraft lignin potential as an alternative for petroleum-based polymers," *Renew. Sustain. Energy Rev.*, vol. 123, p. 109768, 2020, doi: https://doi.org/10.1016/j.rser.2020.109768.

[23] F. R. Vieira, N. Gama, S. Magina, A. Barros-Timmons, D. V Evtuguin, and P. C. O. R. Pinto, "Polyurethane Adhesives Based on Oxyalkylated Kraft Lignin," *Polymers*, vol. 14, no. 23. 2022. doi: 10.3390/polym14235305.

[24] F. R. Vieira *et al.*, "Bio-Based Polyurethane Foams from Kraft Lignin with Improved Fire Resistance," *Polymers*, vol. 15, no. 5. 2023. doi: 10.3390/polym15051074.

[25] X. Wang *et al.*, "Corrosion-resistant polyurethane coatings from structure-homogenized biorefinery lignin through fractionation and oxypropylation," *J. Agric. Food Res.*, vol. 10, p. 100452, 2022, doi: https://doi.org/10.1016/j.jafr.2022.100452.

[26] S. Keck *et al.*, "Synthesis of a Liquid Lignin-Based Methacrylate Resin and Its Application in 3D Printing without Any Reactive Diluents," *Biomacromolecules*, vol. 24, no. 4, pp. 1751–1762, Apr. 2023, doi: 10.1021/acs.biomac.2c01505.

[27] T. Saffar, H. Bouafif, F. L. Braghiroli, S. Magdouli, A. Langlois, and A. Koubaa, "Production of Bio-based Polyol from Oxypropylated Pyrolytic Lignin for Rigid Polyurethane Foam Application," *Waste and Biomass Valorization*, vol. 11, no. 11, pp. 6411–6427, 2020, doi: 10.1007/s12649-019-00876-7.

[28] F. R. Vieira, S. Magina, D. V Evtuguin, and A. Barros-Timmons, "Lignin as a Renewable Building Block for Sustainable Polyurethanes," *Materials*, vol. 15, no. 17. 2022. doi: 10.3390/ma15176182.

[29] I. Kühnel, B. Saake, and R. Lehnen, "Comparison of different cyclic organic carbonates in the oxyalkylation of various types of lignin," *React. Funct.*

Polym., vol. 120, pp. 83–91, Nov. 2017, doi: 10.1016/j.reactfunctpolym.2017.09.011.

[30] J. H. Clements, "Reactive Applications of Cyclic Alkylene Carbonates," *Ind. Eng. Chem. Res.*, vol. 42, no. 4, pp. 663–674, Feb. 2003, doi: 10.1021/ie020678i.

[31] G. Galletti *et al.*, "Glycerol Carbonate as a Versatile Alkylating Agent for the Synthesis of β-Aryloxy Alcohols," *ACS Sustain. Chem. Eng.*, vol. 10, no. 33, pp. 10922–10933, Aug. 2022, doi: 10.1021/acssuschemeng.2c02795.

[32] A. Duval and L. Avérous, "Oxyalkylation of Condensed Tannin with Propylene Carbonate as an Alternative to Propylene Oxide," *ACS Sustain. Chem. Eng.*, vol. 4, no. 6, pp. 3103–3112, Jun. 2016, doi: 10.1021/acssuschemeng.6b00081.

[33] I. Kühnel, B. Saake, and R. Lehnen, "Oxyalkylation of lignin with propylene carbonate: Influence of reaction parameters on the ensuing bio-based polyols," *Ind. Crops Prod.*, vol. 101, pp. 75–83, Jul. 2017, doi: 10.1016/j.indcrop.2017.03.002.

[34] F. R. Vieira, A. Barros-Timmons, D. V. Evtuguin, and P. C. O. R. Pinto, "Oxyalkylation of Lignoboost™ Kraft Lignin with Propylene Carbonate: Design of Experiments towards Synthesis Optimization," *Materials (Basel).*, vol. 15, no. 5, Mar. 2022, doi: 10.3390/ma15051925.

[35] A. Duval, W. Benali, and L. Avérous, "Turning lignin into a recyclable bioresource: transesterification vitrimers from lignins modified with ethylene carbonate," *Green Chem.*, vol. 26, no. 14, pp. 8414–8427, 2024, doi: 10.1039/D4GC00567H.

[36] L.-Y. Liu, K. Bessler, S. Chen, M. Cho, Q. Hua, and S. Renneckar, "In-situ real-time monitoring of hydroxyethyl modification in obtaining uniform lignin derivatives," *Eur. Polym. J.*, vol. 142, p. 110082, 2021, doi: https://doi.org/10.1016/j.eurpolymj.2020.110082.

[37] I. Kühnel, B. Saake, and R. Lehnen, "A New Environmentally Friendly Approach to Lignin-Based Cyclic Carbonates," *Macromol. Chem. Phys.*, vol. 219, no. 7, p. 1700613, Apr. 2018, doi: https://doi.org/10.1002/macp.201700613.

[38] I. Kühnel, J. Podschun, B. Saake, and R. Lehnen, "Synthesis of lignin polyols via oxyalkylation with propylene carbonate," *Holzforschung*, vol. 69, no. 5, pp. 531–538, Jul. 2015, doi: 10.1515/hf-2014-0068.

[39] A. Duval, G. Layrac, A. van Zomeren, A. T. Smit, E. Pollet, and L. Avérous, "Isolation of Low Dispersity Fractions of Acetone Organosolv Lignins to Understand their Reactivity: Towards Aromatic Building Blocks for Polymers Synthesis," *ChemSusChem*, vol. 14, no. 1, pp. 387–397, Jan. 2021, doi: https://doi.org/10.1002/cssc.202001976.

[40] L. Y. Liu, M. Cho, N. Sathitsuksanoh, S. Chowdhury, and S. Renneckar, "Uniform Chemical Functionality of Technical Lignin Using Ethylene Carbonate for Hydroxyethylation and Subsequent Greener Esterification," *ACS Sustain. Chem. Eng.*, vol. 6, no. 9, pp. 12251–12260, Sep. 2018, doi: 10.1021/acssuschemeng.8b02649.

[41] A. Duval and L. Avérous, "Cyclic Carbonates as Safe and Versatile Etherifying Reagents for the Functionalization of Lignins and Tannins," *ACS Sustain. Chem. Eng.*, vol. 5, no. 8, pp. 7334–7343, Aug. 2017, doi: 10.1021/acssuschemeng.7b01502.

[42] L.-Y. Liu, K. Bessler, S. Chen, M. Cho, Q. Hua, and S. Renneckar, "Data on making uniform lignin building blocks via in-situ real-time monitoring of hydroxyethyl modification," *Data Br.*, vol. 33, p. 106512, 2020, doi: https://doi.org/10.1016/j.dib.2020.106512.

[43] Z. Zhang, D. W. Rackemann, W. O. S. Doherty, and I. M. O'Hara, "Glycerol carbonate as green solvent for pretreatment of sugarcane bagasse," *Biotechnol. Biofuels*, vol. 6, no. 1, p. 153, 2013, doi: 10.1186/1754-6834-6-153.

[44] B. Marco-Dufort and M. W. Tibbitt, "Design of moldable hydrogels for biomedical applications using dynamic covalent boronic esters," *Mater. Today Chem.*, vol. 12, pp. 16–33, 2019, doi: https://doi.org/10.1016/j.mtchem.2018.12.001.

[45] Z. Wei *et al.*, "Self-healing gels based on constitutional dynamic chemistry and their potential applications," *Chem. Soc. Rev.*, vol. 43, no. 23, pp. 8114–8131, 2014, doi: 10.1039/C4CS00219A.

[46] L. Terriac, J.-J. Helesbeux, Y. Maugars, J. Guicheux, M. W. Tibbitt, and V. Delplace, "Boronate Ester Hydrogels for Biomedical Applications: Challenges and Opportunities," *Chem. Mater.*, vol. 36, no. 14, pp. 6674–6695, Jul. 2024, doi: 10.1021/acs.chemmater.4c00507.

[47] M. Gosecki and M. Gosecka, "Boronic Acid Esters and Anhydrates as Dynamic Cross-Links in Vitrimers," *Polymers*, vol. 14, no. 4. 2022. doi: 10.3390/polym14040842.

[48] J. N. Cambre and B. S. Sumerlin, "Biomedical applications of boronic acid polymers," *Polymer (Guildf).*, vol. 52, no. 21, pp. 4631–4643, 2011, doi: https://doi.org/10.1016/j.polymer.2011.07.057.

[49] J. A. Peters, "Interactions between boric acid derivatives and saccharides in aqueous media: Structures and stabilities of resulting esters," *Coord. Chem. Rev.*, vol. 268, pp. 1–22, 2014, doi: https://doi.org/10.1016/j.ccr.2014.01.016.

[50] W. L. A. Brooks, C. C. Deng, and B. S. Sumerlin, "Structure–Reactivity Relationships in Boronic Acid–Diol Complexation," *ACS Omega*, vol. 3, no. 12, pp. 17863–17870, Dec. 2018, doi: 10.1021/acsomega.8b02999.

[51] D. Vrbata and M. Uchman, "Preparation of lactic acid- and glucose-responsive poly(ε-caprolactone)-b-poly(ethylene oxide) block copolymer micelles using phenylboronic ester as a sensitive block linkage," *Nanoscale*, vol. 10, no. 18, pp. 8428–8442, 2018, doi: 10.1039/C7NR09427B.

[52] T. Ghosh and A. K. Das, "Dynamic boronate esters cross-linked guanosine hydrogels: A promising biomaterial for emergent applications," *Coord. Chem. Rev.*, vol. 488, p. 215170, 2023, doi: https://doi.org/10.1016/j.ccr.2023.215170.

[53] T. Figueiredo *et al.*, "Injectable Self-Healing Hydrogels Based on Boronate Ester Formation between Hyaluronic Acid Partners Modified with Benzoxaborin Derivatives and Saccharides," *Biomacromolecules*, vol. 21, no. 1, pp. 230–239, Jan. 2020, doi: 10.1021/acs.biomac.9b01128.

[54] X. Meng *et al.*, "Determination of hydroxyl groups in biorefinery resources via quantitative 31P NMR spectroscopy," *Nat. Protoc.*, vol. 14, no. 9, pp. 2627–2647, 2019, doi: 10.1038/s41596-019-0191-1.

[55] Y. Akil, D. Lorenz, R. Lehnen, and B. Saake, "Safe and non-toxic hydroxyalkylation of xylan using propylene carbonate," *Eur. Polym. J.*, vol. 77, pp. 88–97, 2016, doi: https://doi.org/10.1016/j.eurpolymj.2016.02.010.

[56] F. R. Vieira, A. Barros-Timmons, D. V Evtuguin, and P. C. R. Pinto, "Effect of different catalysts on the oxyalkylation of eucalyptus Lignoboost® kraft lignin," vol. 74, no. 6, pp. 567–576, 2020, doi: doi:10.1515/hf-2019-0274.

[57] B. K. Banik, B. Banerjee, G. Kaur, S. Saroch, and R. Kumar, "Tetrabutylammonium Bromide (TBAB) Catalyzed Synthesis of Bioactive Heterocycles," *Molecules*, vol. 25, no. 24. 2020. doi: 10.3390/molecules25245918.

[58] L. C. Over and M. A. R. Meier, "Sustainable allylation of organosolv lignin with diallyl carbonate and detailed structural characterization of modified

lignin," *Green Chem.*, vol. 18, no. 1, pp. 197–207, 2016, doi: 10.1039/C5GC01882J.

[59] S.-C. Kao, Y.-C. Lin, I. Ryu, and Y.-K. Wu, "Revisiting Hydroxyalkylation of Phenols with Cyclic Carbonates," *Adv. Synth. Catal.*, vol. 361, no. 15, pp. 3639–3644, Aug. 2019, doi: https://doi.org/10.1002/adsc.201900287.

[60] Y. Akil, R. Castellani, R. Lehnen, T. Budtova, and B. Saake, "Hydroxyalkylation of xylan using propylene carbonate: comparison of products from homo- and heterogeneous synthesis by HRMAS NMR and rheology," *Cellulose*, vol. 25, no. 1, pp. 217–231, Jan. 2018, doi: 10.1007/s10570-017-1583-4.

[61] A. Duval, D. Vidal, A. Sarbu, W. René, and L. Avérous, "Scalable single-step synthesis of lignin-based liquid polyols with ethylene carbonate for polyurethane foams," *Mater. Today Chem.*, vol. 24, p. 100793, 2022, doi: https://doi.org/10.1016/j.mtchem.2022.100793.

[62] H. K. Chenault, "Introduction to Pyrrolidone and Caprolactam Chemistry," in *Handbook of Pyrrolidone and Caprolactam Based Materials*, 2021, pp. 1–69. doi: https://doi.org/10.1002/9781119468769.hpcbm001.

[63] J.-Y. Kim, H. Hwang, S. Oh, Y.-S. Kim, U.-J. Kim, and J. W. Choi, "Investigation of structural modification and thermal characteristics of lignin after heat treatment," *Int. J. Biol. Macromol.*, vol. 66, pp. 57–65, 2014, doi: https://doi.org/10.1016/j.ijbiomac.2014.02.013.

[64] C. C. Truong, D. K. Mishra, and V. Mishra, "Chapter 13 - Organic carbonate as a green solvent for biocatalysis," Inamuddin, R. Boddula, M. I. Ahamed, and A. M. B. T.-G. S. P. for C. and E. E. and S. Asiri, Eds., Elsevier, 2021, pp. 253–275. doi: https://doi.org/10.1016/B978-0-12-819721-9.00010-8.

[65] L. De Keer *et al.*, "Computational prediction of the molecular configuration of three-dimensional network polymers," *Nat. Mater.*, vol. 20, no. 10, pp. 1422–1430, 2021, doi: 10.1038/s41563-021-01040-0.